CHEMISTRY OF MATERIALS

ARTICLE

pubs.acs.org/cm

Supramolecular Functionalization of Single-Walled Carbon Nanotubes with Triply Fused Porphyrin Dimers: A Study of Structure−Property Relationships

Fuyong Cheng,[†] Jason Zhu,[‡] and Alex Adronov*[,‡]

[†]Steacie Institute for Molecular Sciences, National Research Council Canada, Ottawa, Ontario, Canada

[‡]Department of Chemistry and the Brockhouse Institute for Materials Research, McMaster University, Hamilton, Ontario, Canada

ABSTRACT: A triply fused porphyrin dimer bearing long alkyl chains for enhanced solubility was prepared and investigated for its ability to supramolecularly functionalize single-walled carbon nanotubes. It was found that this porphyrin dimer indeed binds strongly to the nanotube surface, allowing the removal of excess unbound porphyrin from solution without diminishing nanotube solubility. UV−vis spectroscopy indicated a bathochromic shift of the porphyrin Soret band upon binding to the nanotube surface, while Raman spectroscopy indicated that functionalization with the porphyrin dimer does not lead to any defects being formed on the nanotube wall. Transmission electron microscopy revealed the presence of individual nanotubes and small nanotube bundles that were heavily coated with porphyrin dimers. Comparison to analogous fused dimers bearing *tert*-butyl groups for solubility clearly demonstrated that long alkyl chains are necessary for prolonged solution stability of the nanotube complexes. While a previously investigated *tert*-butyl derivative was found to bind to the nanotube surface, the resulting complex precipitated out of solution within minutes. It was also found that the position of bulky substituents on the porphyrin dimer had a dramatic effect on whether it was able to interact with the nanotube surface.

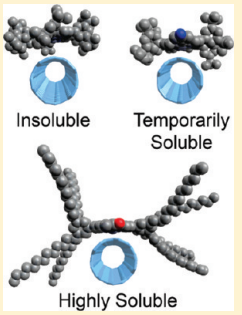

KEYWORDS: triply fused porphyrin dimer, porphyrin synthesis, single-walled carbon nanotube, supramolecular functionalization, structure−property relationships, carbon nanotube solubility

INTRODUCTION

Porphyrins have been extensively investigated in practically all disciplines of science, including chemistry, physics, biology, and medicine.[1] Such immense interest stems from their ability to serve as ligands for a variety of metals,[1] to catalyze a number of reactions,[2] and to absorb and convert light into other forms of energy.[3] Recently, porphyrins have been increasingly investigated as components of nanoscale functional assemblies. In particular, the covalent and supramolecular chemistry of porphyrins with carbon-based materials, such as fullerenes, has received significant attention.[4] In addition, functionalization of carbon nanotubes with porphyrins has been increasingly investigated since interaction of porphyrins with the extended π-electron network of carbon nanotubes leads to complexes with interesting optoelectronic properties.[5−7] The preparation of porphyrin−nanotube conjugates can be achieved through covalent functionalization, such as esterification with oxidized (carboxylic acid-bearing) nanotubes,[8] 1,3-dipolar cycloaddition,[9] diazonium chemistry,[10] and Suzuki coupling to a prefunctionalized nanotube surface.[11] However, all of these covalent methods introduce defect sites on the carbon nanotube sidewall and greatly diminish the stability and conductivity properties of the resulting materials.[12,13]

Conversely, noncovalent functionalization of carbon nanotubes with porphyrins is particularly attractive as it enables the introduction of various porphyrin structures without disturbing the π-system of the nanotube framework.[14] In this approach, significant attention has been given to the use of monomeric porphyrin molecules as supramolecular nanotube adducts.[15−18] In these cases, although the resulting materials could be suspended in solvent by sonication in the presence of excess porphyrin, the complexes were not stable upon removal of the excess unbound porphyrin, indicating that the interaction strength was relatively weak and that an equilibrium between bound and free porphyrin was established. From the perspective of increasing the interaction strength, it is reasonable to expect that multivalent binding, where macromolecular structures bear multiple porphyrin units as side-chains or as polymer backbone components, would be beneficial. To this end, nanotube complexes with PMMA[19] or polypeptide[20] polymers bearing porphyrins as side chains have been prepared and were found to be relatively soluble in polar organic solvents, such as DMF.

Conjugated porphyrin polymers containing butadiyne bridges linked directly to the porphyrin meso carbons are fully conjugated, rigid, and strongly electron-donating structures.[21−23] These properties make conjugated porphyrin polymers highly complementary to the conjugated, rigid, but electron-accepting SWNTs. It was therefore feasible that the interaction between SWNTs and conjugated porphyrin polymers would be much stronger than the analogous interaction with monomeric porphyrins. Recently, we have found that such polymers indeed form strong interactions with the nanotube surface in THF.[24,25] Unfortunately, structural flexibility within the polymer backbone

Received: February 14, 2011
Revised: May 24, 2011
Published: June 14, 2011

dx.doi.org/10.1021/cm2004648 | *Chem. Mater.* 2011, 23, 3188–3194

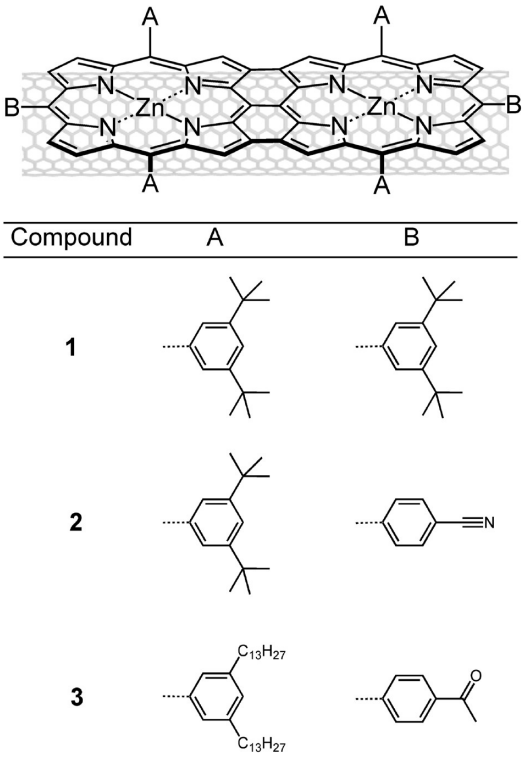

Figure 1. General structure of the triply fused porphyrin dimer superimposed on the structure of a carbon nanotube (top, not to scale) and the chemical structures of the substituents on the three porphyrin dimers (**1**, **2**, and **3**) used in this study (bottom).

limited the binding strength to nanotubes and allowed equilibration between bound and unbound polymers.[24]

To increase the nanotube interaction strength, we recently turned to triply fused Zn(II)-porphyrin oligomers, in which each repeat unit is absolutely restricted to a fully coplanar orientation with its neighbor.[26−28] This coplanarity produces "molecular tapes" that exhibit enhanced conjugation and greater electron-donating ability relative to those of all other porphyrin oligomers and polymers. These triply fused oligomers were therefore deemed ideal candidates for strong supramolecular interactions with SWNTs. In our recent work, we investigated the nanotube binding strength of *tert*-butyl-functionalized triply fused porphyrin dimer and trimer molecules,[29] relative to the analogous monomeric control compound, and found that the trimer alone formed extremely strong and nearly irreversible supramolecular interactions with SWNTs, leading to stable solutions.[29] Interestingly, in the case of the dimer, we found that a highly concentrated homogeneous solution could be formed upon sonication, but the complexes precipitated on standing for several hours. We therefore hypothesized that either the binding strength between the dimer and the nanotubes is too low to impart long-term solution stability or the *tert*-butyl groups in this structure do not provide enough solubility to keep the nanotube−porphyrin complexes in solution. In order to answer this question, we have undertaken the synthesis and investigation of a triply fused porphyrin dimer that is functionalized with *n*-tridecyl chains for enhanced solubility. Here, we compare the nanotube binding and solubilizing ability of this new porphyrin dimer to that of two previously reported analogous structures (Figure 1).

RESULTS AND DISCUSSION

Three different triply fused porphyrin dimers, **1**, **2**, and **3**, were investigated as part of this study (structures shown in Figure 1). These three structures differ in the substituent types that are located at the two different meso positions, labeled A and B (Figure 1). Compound **1** exhibits only bulky 3,5-di-*tert*-butylphenyl substituents, while compound **2** is functionalized with 3,5-di-*tert*-butylphenyl at positions A and the less sterically demanding 4-cyanophenyl substituents at positions B. Both of these structures were synthesized according to literature procedures.[29,30] Dimer **3** is functionalized with 3,5-di-*n*-tridecylphenyl substituents at positions A for enhanced solubility and 4-(1-oxyethyl)-phenyl as sterically nondemanding substituents in the B positions. The synthetic approach for the preparation of porphyrin dimer **3** is shown in Scheme 1. Briefly, treatment of commercially available 5-bromo-*m*-xylene with NBS resulted in 1-bromo-3,5-bis(bromomethyl) benzene, which was reacted with $P(OMe)_3$ to give diphosphonate **5**. Subsequent treatment of **5** with dodecyl aldehyde via the Horner−Wadsworth−Emmons reaction, followed by hydrogenation in the presence of palladium/carbon catalyst, afforded 1-bromo-3,5-di-*n*-tridecylbenzene (**7**). Phenyl bromide **7** was then reacted with BuLi and DMF to produce the long alkyl chain substituted benzaldehyde **8** (24% yield over five steps). Condensation of aldyhede **8** with dipyrromethane and metalation with Zn(II) acetate afforded Zn-porphyrin **10**. Porphyrin **10** was then treated with one equivalent of NBS, yielding porphyrin bromide **11**, which was reacted with the phenylboronic ester **12** by Pd-catalyzed Suzuki cross-coupling to give the porphyrin derivative **13**. Porphyrin monomer **13** was then converted into the triply fused dimer **3** in one step using the oxidative ring closure mediated by DDQ and $Sc(OTf)_3$.[30]

Our recent work has shown that a solution of THF containing 5% TFA is a good solvent medium to form and solubilize the Zn-porphyrin polymer and triply fused porphyrin oligomer complexes with SWNTs.[24,29] In the present work, this solvent system was again used for the investigation of supramolecular interactions between the three porphyrin dimers and SWNTs. In a typical experiment, a HiPco SWNT sample (1.0 mg) was added to separate solutions of porphyrin dimers **1**, **2**, and **3** in the THF/TFA solution (0.4 mg/mL), and the mixture was sonicated for 1 h. The resulting nanotube suspension was filtered through a 200 nm pore-diameter Teflon membrane and washed repeatedly with the 5% TFA in THF solution until all the excess porphyrin dimer was removed, as indicated by the complete loss of color in the filtrate. The remaining residue was then resuspended in 5 mL of the 5% TFA/THF solution by sonicating for 5 min. When this procedure was carried out with dimer **1**, sonication of the residue did not result in any observable SWNT solubility, indicating that the washing procedure likely removed all the porphyrin dimers, and no significant interaction between **1** and the SWNTs exists. In contrast, when the same procedure was carried out with a solution of dimer **2**, sonication of the washed nanotube residue resulted in the initial formation of a homogeneous solution. However, as observed previously,[29] upon standing for several hours, the SWNTs were found to completely precipitate, leaving a clear, colorless supernatant. Conversely, when the nanotubes were added to a solution of dimer **3**, and the above procedure was again repeated, a very stable, dark solution was obtained after sonication of the washed residue for 5 min. This solution remained stable upon standing indefinitely, and no sedimentation was observed even after centrifugation for 20 min at 2576*g*.

Scheme 1. Synthesis of Porphyrin Dimer 3[a]

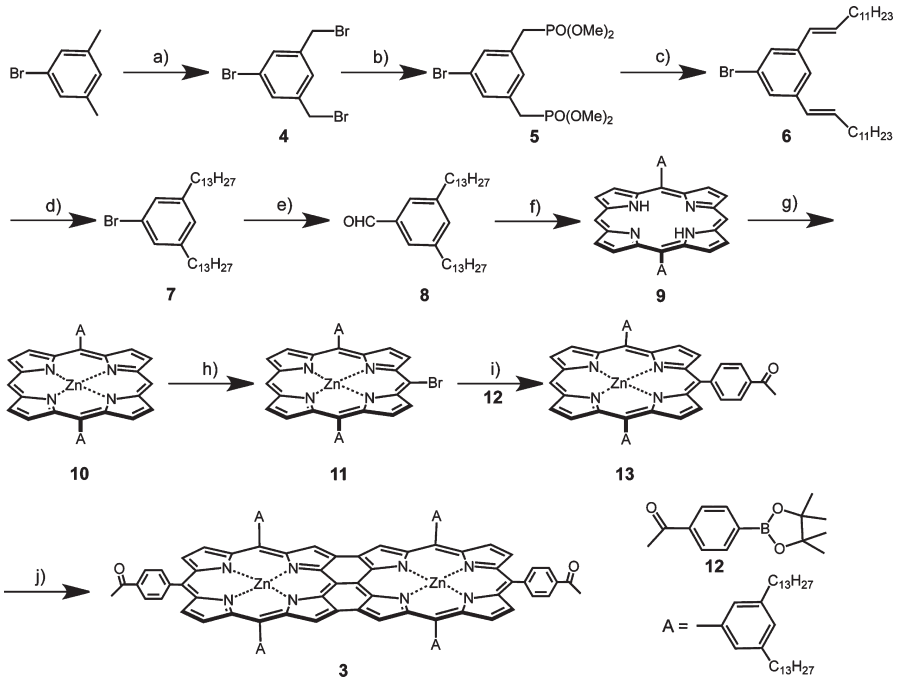

[a] Conditions: (a) NBS, CCl_4, 30%; (b) $P(OMe)_3$, 100%; (c) $C_{11}H_{23}CHO$, NaH, THF, 85%; (d) Pd/C, H_2, THF, 100%; (e) BuLi, THF, DMF, 97%; (f) dipyrromethane, TFA, DDQ, CH_2Cl_2, 4%; (g) $Zn(OAc)_2$, $CHCl_3$/MeOH, 95%; (h) NBS, CH_2Cl_2/pyridine; (i) **12**, $Pd(PPh_3)_4$, Cs_2CO_3, toluene, 73% (over two steps); (j) DDQ, $Sc(OTf)_3$, toluene, 60%.

These observations can be explained by considering the position and structure of the substituents on the porphyrin dimer. To maximize π-stacking interactions, it is expected that the porphyrin dimer would preferentially orient its long axis along the length of the SWNT structure (Figure 1). In this configuration, large solubility-enhancing substituents bound to the porphyrin *meso*-carbons at the two ends (positions B) can actually prevent the close interaction of the dimer with the nanotube surface that is necessary for the π-stacking interaction to be significant. Conversely, large substituents that are present at the sides of the porphyrin dimer (positions A) will not hinder π-stacking and will only serve to impart solubility to the overall structure. It is therefore not surprising that dimer **1**, which bears the bulky 3,5-di-*tert*butylphenyl groups at both ends, does not exhibit any significant interaction with the SWNT wall and cannot impart even temporary solubility to the **1**-SWNT complex. The structure of **2**, which only differs from that of dimer **1** by the linear and relatively nonsterically encumbered *p*-cyanophenyl groups at its two ends, leads to a temporary solubilization of the **2**-SWNT complex. This is understandable because the two end groups do not hinder the π-stacking interactions between the porphyrin dimer and the SWNT surface, allowing the formation of a stable complex. However, in this structure, the flanking 3,5-di-*tert*-butylphenyl groups that were installed to impart solubility are only temporarily effective in this role. Upon sonication, nanotube solubility is observed, but the **2**-SWNT complexes precipitate over time as the *t*-butyl solubilizing groups are too rigid and not effective enough in permanently stabilizing the complexes in solution. However, the structure of dimer **3** exhibits both types of necessary substituents for maximal nanotube interactions and solubility enhancement. The relatively small and unencumbered 4-acetylphenyl substituents present at the two ends do not hinder

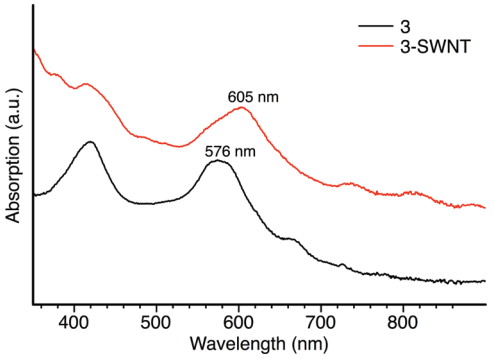

Figure 2. UV−vis spectra of porphyrin dimer **3** (black) and the **3**-SWNT complex (red).

close π-stacking interactions with SWNTs, while the multiple flexible tridecyl chains significantly enhance the solubility of the **3**-SWNT complex, to the point that the complexes remain stable in solution indefinitely. It should be noted that a previously described monomeric porphyrin unit with long alkyl side-chains,[24] analogous to those discussed above, was found to not impart any solubility to SWNTs. Thus, a balance between the extended π-conjugation of the porphyrin oligomers and the size of solubilizing side chains must be achieved in order to impart a high degree of solubility to the porphyrin−SWNT complexes. As the oligomer gets shorter, the side chain must become longer, and vice versa.

The supramolecular interaction of dimer **3** with SWNTs was investigated by UV−vis absorption spectroscopy. Figure 2 depicts the UV−vis absorption spectra of dimer **3** and the **3**-SWNT complex in acidified THF. Upon complexation of the dimer to

dx.doi.org/10.1021/cm2004648 |*Chem. Mater.* 2011, 23, 3188–3194

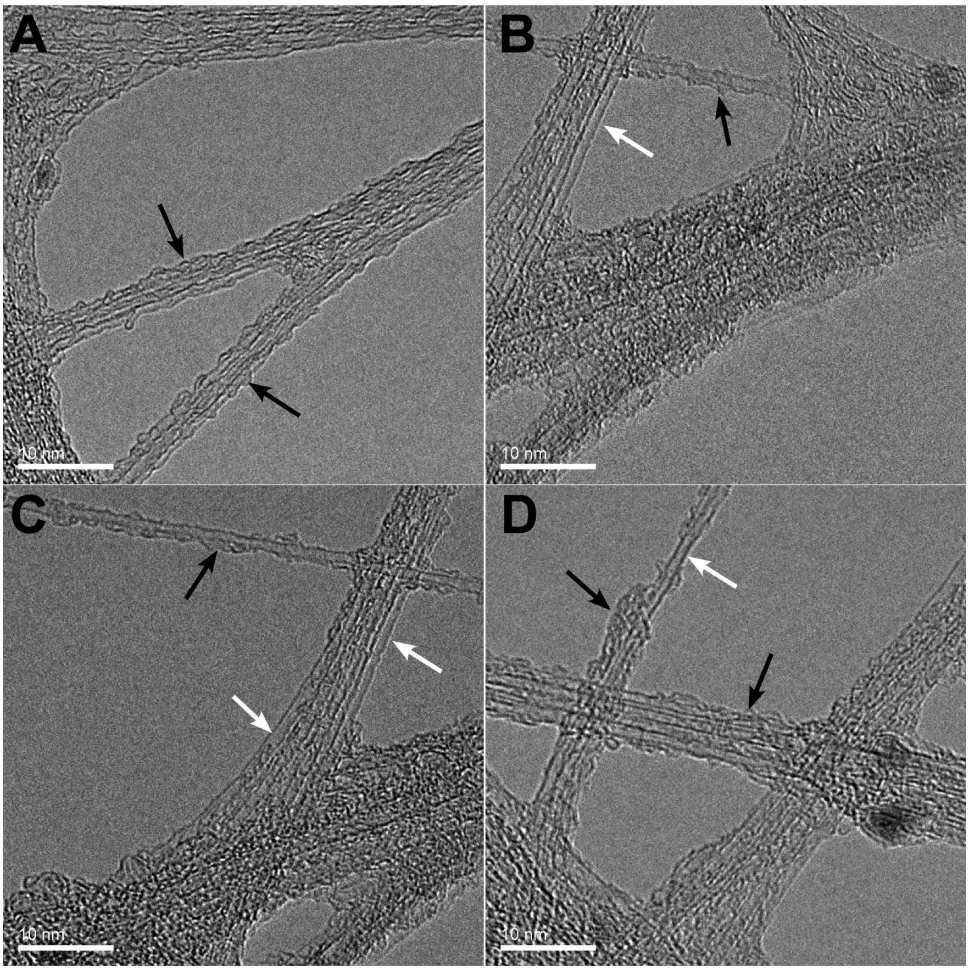

Figure 3. Representative TEM images of the **3**-SWNT complex deposited from solution. Arrows indicate several positions of dimer-functionalized nanotube sections (black arrows) and sections of bare nanotubes (white arrows). Most of the nanotube area is covered by the porphyrin dimer. Scale bars correspond to 10 nm.

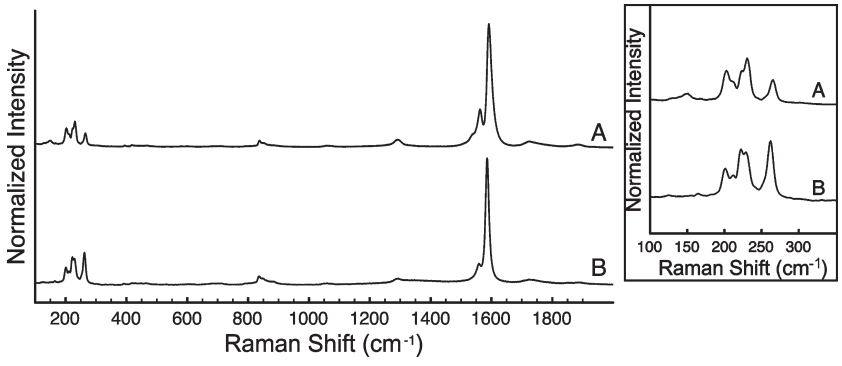

Figure 4. Raman spectra of pristine SWNTs (A) and the **3**-SWNT complex. The inset shows a close-up of the spectral region between 100 and 350 cm^{-1}, corresponding to the radial breathing mode (RBM) region.

SWNTs, a bathochromic shift relative to the dimer alone was observed. The longer wavelength component of the split Soret band was observed to shift from 576 to 603 nm. The shift in the absorption spectra upon oligoporphyrin complexation to SWNTs is a clear manifestation of electronic interactions between the porphyrins and the nanotubes, possibly signifying a porphyrin-to-nanotube electron transfer.

Further characterization of the **3**-SWNT complex was accomplished by transmission electron microscopy (TEM). A drop of the **3**-SWNT solution, prepared as described above, was placed on a holey carbon coated copper TEM grid and was allowed to air-dry prior to loading into the microscope. Figure 3 shows four representative images of the sample, indicating the presence of long fiber-like structures that are mostly coated along their length

dx.doi.org/10.1021/cm2004648 |*Chem. Mater.* 2011, 23, 3188–3194

with organic material. These structures clearly resemble exfoliated carbon nanotubes and small nanotube bundles that have been heavily coated with the porphyrin dimer **3** (indicated by black arrows). A few areas where individual uncoated nanotubes can be seen are indicated by white arrows (Figure 3).

Additional characterization of the **3**-SWNT complexes was accomplished by Raman spectroscopy with excitation at 785 nm. The characteristic absorptions at ~1590 cm^{-1}, ~1300 cm^{-1}, and 150−300 cm^{-1}, corresponding to the graphitic (G) band, the disorder (D) band, and the radial breathing modes (RBMs) of SWNTs, respectively, are clearly visible (Figure 4, curve B). A comparison to pristine, unfunctionalized SWNTs (Figure 4, curve A) revealed only a few differences. First, the line shape of the G band of **3**-SWNT shows a slightly decreased G^- band (~1560 cm^{-1}) relative to the pristine sample of SWNTs, indicating a lower concentration of metallic nanotubes.[31] Similarly, the D band has a slightly lower intensity in **3**-SWNT, indicating that functionalization with porphyrin dimer **3** does not lead to any defects being formed on the nanotube wall, as expected for supramolecular functionalization. Finally, close examination of the RBM signals of **3**-SWNT indicates that signals at ~260 and ~220 cm^{-1} are increased in intensity relative to the other signals of pristine SWNTs, while the small signal at 150 cm^{-1}, present in the pristine nanotubes, is undetectable in **3**-SWNT (Figure 4, inset). These signals could be interpreted to indicate a slight preference of the dimer for specific nanotube diameters,[32−34] but it is difficult to make conclusions with these polydisperse, surface-functionalized SWNT samples. Surface functionalization can shift peak positions, and can change the nanotube types that are in resonance with the excitation wavelength.

CONCLUSIONS

This work demonstrates that triply fused porphyrin dimers can exhibit strong interactions with the nanotube surface, leading to prolonged solution stability, as long as they are appropriately functionalized. To impart the observed solubility, large solubilizing groups (long alkyl chains) must be installed along the long axis of the dimer structure. However, sterically bulky substituents at the two ends (along the short axes) of the triply fused dimer hinder the close interaction of the porphyrin with the nanotube surface and should be avoided. In the present case, tridecyl chains along the long axis and methyl phenyl ketone groups along the short axis successfully provided the desired interaction strength and nanotube solubility. It was found that excess porphyrin dimer could be removed by ultrafiltration and excessive washing with THF, resulting in a residue that retained its solubility. TEM analysis revealed the presence of individual nanotubes and small nanotube bundles that were heavily coated with porphyrin molecules, while UV−vis spectroscopy indicated that the porphyrin Soret band exhibits a bathochromic shift upon nanotube complexation. Detailed Raman analysis indicated that complexation of nanotubes by the porphyrin strucures does not lead to any structural changes to the nanotubes.

EXPERIMENTAL SECTION

General. Single-walled carbon nanotubes (SWNTs) were purchased from Carbon Nanotechnologies, Inc. (Houston, TX). All other reagents were purchased from commercial suppliers and used as received. TEM analysis was performed using JEOL 2010F operating at 200 keV. NMR was performed on a Bruker 200, 500, or 600 MHz instrument. FTIR was performed on a BIO-RAD FTS-40 instrument. UV−vis spectra were measured using a Cary 50 UV−visible spectrophotometer. High resolution ESI-MS measurements were done on the Micromass Ultima Global instrument (quadrupole time-of-flight), and MALDI−MS was performed on the Waters/Micromass MALDI Micro instrument (α-cyano-4-hydroxycinnamic acid as matrix). Raman spectroscopy was performed on a Renishaw InVia Raman spectrometer equipped with a 25 mW argon ion laser (514 nm), a 300 mW Renishaw 785 nm laser, and 1800 L/mm and 1200 L/mm gratings for the two lasers, respectively. The Raman system also is equipped with a Leica microscope having 5×, 20×, and 50× objectives as well as a USB camera for sample viewing. The 785 nm laser was operated at 5% intensity to avoid damage to the sample. Ultrasonication was done in a Branson Ultrasonics B1510 bath sonicator. Filtration was done through a 200 nm-pore Teflon membrane (Millipore).

Synthesis of 1-Bromo-3,5-bis(bromomethyl) Benzene (4). 5-Bromo-*m*-xylene (34.94 g, 0.19 mol), *N*-bromo-succinimide (70.57 g, 0.40 mol), and benzoyl peroxide (0.5 g, 2.1 mmol) were added to dry CCl_4 (300 mL) in a 500 mL round-bottom flask, equipped with a stir bar and a reflux condenser, under Ar. The reaction was then heated to reflux in the dark and stirred for 16 h. The mixture was filtered through a fritted funnel, and the filtrate was evaporated *in vacuo*. Recrystallization from the minimum amount of hexanes afforded the desired product **4** as a white solid (19.43 g, 30%). ^{1}H NMR ($CDCl_3$, 200 MHz): δ 4.40 (s, 4 H), 7.33 (s, 1 H), 7.46 (s, 2 H). ^{13}C NMR ($CDCl_3$, 50 MHz): δ 31.44, 122.67, 128.23, 131.94, 140.27. IR (KBr, cm^{-1}): 1580 (m), 1445 (m), 1262 (m), 1212 (s), 878 (m), 864 (m), 818 (w), 691 (s), 602 (s), 586 (m), 539 (s), 484 (w). HRMS (EI) *m*/*z* calcd for $C_8H_7Br_3$ (M^+) 339.8098; found, 339.8085.

Synthesis of Tetramethyl [(5-Bromo-1,3-phenylene)bis-(methylene)]bis-phosphonate (5). Compound **4** (18.27 g, 53.29 mmol) was added to trimethyl phosphite (200 mL) in a 500 mL round-bottom flask, equipped with a stir bar and a reflux condenser, under inert Ar atmosphere. The reaction was heated to reflux for 16 h, then the mixture was cooled, and the phosphite was removed *in vacuo*. The desired product **5** was obtained as a white solid (21.61 g, 100%). ^{1}H NMR ($CDCl_3$, 200 MHz): δ 3.07 (d, 4 H, J = 22.0 Hz), 3.68 (d, 12 H, J = 10.8 Hz), 7.15 (s, 1 H), 7.32 (s, 2 H). ^{13}C NMR ($CDCl_3$, 50 MHz): δ 30.93, 33.68, 52.82, 52.96, 122.53, 129.74, 131.25, 133.62. IR (KBr, cm^{-1}): 2952 (w), 2916 (w), 1569 (w), 1444 (w), 1240 (s), 1224 (m), 1050 (s), 1032 (s), 863 (m), 835 (w), 805 (w), 724 (w), 688 (m), 556 (w), 537 (w). HRMS (EI) *m*/*z* calcd for $C_{12}H_{19}BrO_6P_2$ (M^+) 399.9840; found, 399.9823.

Synthesis of 1-Bromo-3,5-di-1-tridecenyl-benzene (6). Dodecyl aldehyde (39.48 g, 0.21 mol) and NaH (40 g, 1.67 mol) were added to THF (250 mL) in a 500 mL three-neck round-bottom flask, equipped with a stir bar, an addition funnel, and a reflux condenser, under inert Ar atmosphere. Diphosphonate **5** (21.50 g, 53.57 mmol) was dissolved in THF (150 mL), transferred to the funnel, and added dropwise to the reaction vessel. After heating at reflux for 16 h, water (50 mL) was added dropwise to the mixture until effervescence subsided. THF was removed *in vacuo*. Organic compounds were extracted into hexanes (100 mL) and subsequently washed with water (3 × 100 mL). Hexane was removed *in vacuo*. The desired product **6** was obtained as a white solid (23.64 g, 85%). ^{1}H NMR ($CDCl_3$, 200 MHz): δ 0.88 (t, 6 H, J = 6.5 Hz), 1.27 (m, 36 H), 2.20 (m, 4 H), 6.26−6.24 (m, 4 H), 7.17 (s, 1 H), 7.30 (s, 2 H). ^{13}C NMR ($CDCl_3$, 50 MHz): δ 14.12, 22.68, 29.22, 29.64, 31.91, 33.00, 122.45, 122.83, 126.86, 128.40, 132.81, 139.98. IR (KBr, cm^{-1}): 2924 (s), 2853 (s), 1706 (w), 1464 (m), 963 (w). HRMS (EI) *m*/*z* calcd for $C_{32}H_{53}Br$ (M^+) 516.3331; found, 516.3322.

Synthesis of 1-Bromo-3,5-di-*n*-tridecyl-benzene (7). Compound **6** (23.64 g, 45.65 mmol) and palladium/carbon catalyst (0.5 g) were added to THF (200 mL) in a 500 mL round-bottom flask,

equipped with a stir bar, under inert Ar atmosphere. The mixture was stirred vigorously at room temperature (22 °C) for 20 h. The mixture was then filtered through Celite and then silica, washing with THF (3 × 20 mL). THF was removed *in vacuo*. The target product **7** was obtained as a white solid (23.62 g, 100%). ^{1}H NMR ($CDCl_3$, 200 MHz): δ 0.88 (t, 6 H, J = 6.1 Hz), 1.25 (m, 40 H), 1.57 (m, 4 H), 2.52 (t, 2 H, J = 7.7 Hz), 6.89 (s, 1 H), 7.12 (s, 2 H). ^{13}C NMR ($CDCl_3$, 50 MHz): δ 14.13, 22.68, 29.66, 31.32, 31.59, 31.93, 35.63, 127.34, 128.59, 144.97. IR (KBr, cm^{-1}): 2924 (s), 2853 (s), 1600 (w), 1569 (m), 1464 (m). HRMS (EI) m/z calcd for $C_{32}H_{57}Br$ (M^+) 520.3644; found, 520.3626.

Synthesis of 3,5-Di-*n*-tridecyl-benzaldehyde (8). Compound **7** (23.00 g, 44 mmol) was added to THF (200 mL) in a 500 mL round-bottom flask, equipped with a stir bar, under inert Ar atmosphere and cooled to −60 °C. While stirring, BuLi (60 mL, 2.5 M in hexane, 150 mmol) was added dropwise. After 30 min, DMF (20 mL) was added dropwise. The mixture was warmed to room temperature. After 2 h, 5 vol % H_2SO_4 (50 mL) was added. CH_2Cl_2 (500 mL) was added to the mixture, which was then washed with brine. CH_2Cl_2 was then removed *in vacuo*. The product was purified by column chromatography on silica gel using hexanes as the initial eluent and then switching to CH_2Cl_2. The solvent was then removed *in vacuo*. The target product **8** was obtained as a white solid (19.50 g, 94%). ^{1}H NMR (CD_2Cl_2, 200 MHz): δ 0.87 (t, 6 H, J = 7.7 Hz), 1.27 (m, 40 H), 1.61 (m, 4 H), 2.65 (t, 2 H, J = 7.7 Hz), 7.27 (s, 1 H), 7.49 (s, 2 H), 9.94 (s, 1 H). ^{13}C NMR ($CDCl_3$, 50 MHz): δ 22.68, 29.25, 29.35, 29.45, 29.65, 31.31, 31.91, 35.61, 127.12, 134.99, 136.62, 143.80, 192.81. IR (KBr, cm^{-1}): 2918 (s), 2850 (s), 1697 (m), 1595 (w), 1465 (m), 1142 (m), 721 (w). HRMS (EI) m/z calcd for $C_{33}H_{58}O$ (M^+) 470.4488; found, 470.4491.

Synthesis of 5,15-Bis(3,5-di-*n*-tridecylphenyl)-porphyrin (9). Aldehyde **8** (1.94 g, 4.13 mmol) and dipyrromethane (0.6 g, 4.11 mmol) were added to deaerated CH_2Cl_2 (1 L) in a 2 L round-bottom flask, equipped with a stir bar, under inert Ar atmosphere. TFA (0.3 mL) was added, and the reaction was stirred in the dark for 16 h at room temperature. DDQ (3.1 g, 13.65 mmol) and triethylamine (1.0 mL) were then added, and the solution was stirred for a further 2 h. CH_2Cl_2 was removed *in vacuo*. The product was first roughly isolated by column chromatography on silica gel using a mixture of hexanes/CH_2Cl_2 (1:1) as the eluent, then finely purified using a second round of column chromatography on silica gel using a mixture of hexanes/CH_2Cl_2 (5:1) as the eluent. The solvent was then removed *in vacuo*. The desired product **9** was obtained as a purple solid (200 mg, 4%). ^{1}H NMR ($CDCl_3$, 200 MHz): δ −3.08 (s, 2 H), 0.86 (t, 12 H, J = 6.4 Hz), 1.27 (m, 40 H), 1.90 (m, 8 H), 2.92 (t, 8 H, J = 7.6 Hz), 7.45 (s, 2 H), 7.93 (s, 4 H), 9.14 (d, 4 H, J = 4.7 Hz), 9.39 (d, 4 H, J = 4.7 Hz), 10.30 (s, 2 H). ^{13}C NMR ($CDCl_3$, 50 MHz): δ 14.16, 22.73, 29.70, 31.85, 31.96, 36.09, 105.08, 119.77, 127.91, 131.17, 131.40, 132.92, 141.04, 141.30, 145.08, 147.29. IR (KBr, cm^{-1}): 2922 (s), 2851 (s), 1632 (m), 1590 (w), 1435 (m), 1162 (m), 731 (w). UV−vis ($CHCl_3$, λ_{max}, nm): 436, 574, 625, 674. HRMS (ESI) m/z calcd for $C_{84}H_{127}N_4$ (M^+) 1192.0061; found, 1191.9993.

Synthesis of [5,15-Bis(3,5-di-*n*-tridecylphenyl)-porphyrinato(2−)-$\kappa N^{21},\kappa N^{22},\kappa N^{23},\kappa N^{24}$] Zinc(II) (10). A solution of Zn(OAc)$_2$·2H$_2$O (1.16 g, 5.3 mmol) in methanol (20 mL) was added to a solution of porphyrin **9** (520 mg, 0.44 mmol) in $CHCl_3$ (40 mL) in a 100 mL round-bottom flask, equipped with a stir bar. The solution was stirred in the dark at room temperature overnight. The organic layer was washed with water (3 × 30 mL) and dried over Na_2SO_4. The product was purified by column chromatography on silica gel using a mixture of hexanes/CH_2Cl_2 (5:1) as the eluent. The target product **10** was obtained as a dark pink solid (550 mg, 100%). ^{1}H NMR ($CDCl_3$, 200 MHz): δ 0.86 (t, 12 H, J = 6.3 Hz), 1.25 (m, 40 H), 1.88 (m, 8 H), 2.87 (t, 8 H, J = 7.5 Hz), 7.43 (s, 2 H), 7.90 (s, 4 H), 9.17 (d, 4 H, J = 4.7 Hz), 9.44 (d, 4 H, J = 4.7 Hz), 10.30 (s, 2 H). ^{13}C NMR ($CDCl_3$, 50 MHz): δ 14.18, 22.73, 29.70, 30.33, 31.84, 31.96, 34.21, 36.10, 105.07, 119.76, 125.56, 127.13, 127.92, 128.75, 131.15, 131.38, 132.94, 141.06, 141.29, 145.08, 147.32. IR (KBr, cm^{-1}): 2923 (s), 2852 (s), 1596 (m), 1464 (m), 1392 (w), 1059 (m), 994 (m), 848 (m), 782 (m), 726 (w). UV−vis ($CHCl_3$, λ_{max}, nm): 436, 627. MALDI-TOF-MS m/z calcd for $C_{84}H_{124}N_4Zn$ (M^+) 1252.9117; found, 1252.90.

Synthesis of [10,20-Bis(3,5-di-*n*-tridecylphenyl)-5-bromo-porphyrinato(2−)-$\kappa N^{21},\kappa N^{22},\kappa N^{23},\kappa N^{24}$]zinc(II) (11). Zn-porphyrin **10** (250 mg, 0.20 mmol) and pyridine (0.3 mL) were added to CH_2Cl_2 (30 mL) in a 100 mL round-bottom flask, equipped with a stir bar. The solution was cooled to 0 °C and NBS (39 mg, 0.22 mmol) was added under inert Ar atmosphere. After 10 min, the reaction was quenched with acetone (4 mL), and the solvent was removed *in vacuo*. The residue was washed with methanol (3 × 50 mL) and dried *in vacuo*. A mixture of unbrominated, monobrominated, and dibrominated porphyrin was obtained as a purple solid (290 mg) and used directly in the Suzuki coupling reaction without product isolation.

Synthesis of 2-(4-Acetylphenyl)-4,4,5,5-tetramethyl-1,3,2-dioxaborolane (12). Pinacol (10.81 g, 92 mmol) and 4-acetylphenylboronic acid (5 g, 31 mmol) were added to ethyl ether (150 mL) in a 250 mL round-bottom flask, equipped with a stir bar. The reaction was stirred for 16 h at room temperature. The mixture was then washed with water (5 × 100 mL) to remove excess pinacol, and ether solvent was removed *in vacuo*. The target product **12** was obtained as a pale yellow solid (6.72 g, 90%). ^{1}H NMR (CD_2Cl_2, 200 MHz): δ 1.35 (s, 12 H), 2.61 (s, 3 H), 7.87 (d, 2 H, J = 8.3 Hz), 7.93 (d, 2 H, J = 8.1 Hz). ^{13}C NMR ($CDCl_3$, 50 MHz): δ 24.78, 26.65, 84.10, 127.17, 134.83, 138.90, 198.27. IR (KBr, cm^{-1}): 2980 (m), 1684 (s), 1555 (w), 1507 (m), 1397 (s), 1358 (s), 1265 (s), 1214 (w), 1142 (m), 1094 (m), 1015 (w), 961 (w), 857 (m), 827 (w), 731 (w), 655 (m), 670 (m), 599 (w). HRMS (EI) m/z calcd for $C_{14}H_{19}BO_3$ (M^+) 246.1427; found, 246.1433.

Synthesis of [10,20-Bis(3,5-di-*n*-tridecylphenyl)-5-(4-acetylphenyl)porphyrinato(2−)-$\kappa N^{21},\kappa N^{22},\kappa N^{23},\kappa N^{24}$]zinc(II) (13). The bromo-porphyrin mixture **11** (290 g), borate **12** (160 mg, 0.651 mmol), and $CsCO_3$ (0.7 g, 2.17 mmol) were added to toluene (60 mL) in a 100 mL round-bottom flask, equipped with a stir bar, and deaerated under inert Ar atmosphere by sonication for 40 min. The solution was then heated to reflux and stirred for 16 h. TLC revealed three distinct products. The solution was then filtered through a Celite plug and washed with toluene (3 × 15 mL). The solvent was removed from the filtrate *in vacuo*. The products were purified by column chromatography on silica gel. Hexanes/CH_2Cl_2 (5:1) was used to elute the unfunctionalized porphyrin, hexanes/CH_2Cl_2 (2:1) eluted the monofunctionalized porphyrin, and pure CH_2Cl_2 eluted the difunctionalized porphyrin. The combined two-step process of porphyrin bromination and Suzuki coupling afforded the monofunctionalized porphyrin **13** as a red solid (200 mg, 73%) and difunctionalized porphyrin **14** as a purple solid (70 mg, 23%). Data for **13**: ^{1}H NMR ($CDCl_3$, 200 MHz) δ 0.83 (t, 12 H, J = 6.3 Hz), 1.21 (m, 40 H), 1.84 (m, 8 H), 2.85 (s, 3 H), 2.85 (t, 8 H, J = 7.5 Hz), 7.40 (s, 2 H), 7.87 (s, 4 H), 8.31 (s, 4 H), 8.89 (d, 2 H, J = 4.6 Hz), 9.03 (d, 2 H, J = 4.8 Hz) 9.13 (d, 2 H, J = 4.8 Hz), 9.38 (d, 2 H, J = 4.4), 10.24 (s, 1 H). ^{13}C NMR ($CDCl_3$, 50 MHz): δ 14.13, 22.70, 26.52, 29.67, 31.93, 36.09, 105.77, 119.44, 121.37, 126.34, 127.72, 131.23, 131.52, 132.31, 132.68, 134.58, 135.69, 140.87, 142.25, 148.39, 148.93, 149.59, 150.25, 198.29. IR (KBr, cm^{-1}): 2923 (s), 2852 (s), 1688 (m), 1597 (w), 1465 (m), 1263 (w), 995 (m), 791 (w), 717 (w). UV−vis ($CHCl_3$, λ_{max}, nm): 444, 642. MALDI-TOF-MS m/z calcd for $C_{92}H_{130}N_4OZn$ (M^+) 1370.9536; found, 1370.93.

Data for [5,15-Bis(4-acetylphenyl)-10,20-bis(3,5-di-*n*-tridecylphenyl)porphyrinato(2−)-$\kappa N^{21},\kappa N^{22},\kappa N^{23},\kappa N^{24}$]zinc(II) (14). ^{1}H NMR ($CDCl_3$, 200 MHz): δ 0.86 (t, 12 H, J = 6.7 Hz), 1.23 (m, 40 H), 1.87 (m, 8 H), 2.75 (s, 6 H), 2.89 (t, 8 H, J = 7.2 Hz), 7.43 (s, 2 H), 7.90 (s, 4 H), 8.24 (d, 4 H, J = 8.1 Hz), 8.34 (d, 4 H, J = 8.0 Hz) 8.91 (d, 4 H, J = 4.7 Hz), 9.05 (d, 4 H, J = 4.7). ^{13}C NMR ($CDCl_3$, 50 MHz): δ 14.10, 22.67, 26.76, 29.34, 29.67, 31.76, 31.89, 36.65, 122.32, 126.49,

dx.doi.org/10.1021/cm2004648 |*Chem. Mater.* 2011, 23, 3188–3194

127.85, 131.45, 132.54, 134.58, 136.03, 140.90, 142.24, 148.08, 149.55, 150.53, 198.24. IR (KBr, cm^{-1}): 2923 (s), 2852 (s), 1687 (m), 1659 (m), 1598 (s), 1465 (w), 1265 (m), 1070 (w), 997 (m) 795 (w), 717 (m). UV−vis ($CHCl_3$, λ_{max}, nm): 452, 667. MALDI-TOF-MS m/z calcd for $C_{100}H_{136}N_4O_2Zn$ (M^+) 1488.9955; found, 1488.93.

Synthesis of {μ-[10,10′-Bis(4-acetylphenyl)-5,5′,15,15′-tetrakis(3,5-di-*n*-tridecylphenyl)-18,18′:20,20′-dicyclo-2,2′-biporphyrinato(4−)-κN^{21},κN^{22},κN^{23},κN^{24}:$\kappa N^{21'}$,$\kappa N^{22'}$,$\kappa N^{23'}$,$\kappa N^{24'}$]} Dizinc(II) (3). The monofunctionalized porphyrin (50 mg, 0.036 mmol), Sc(OTf) (90 mg, 0.182 mmol), and DDQ (41 mg, 0.182 mmol) were added to dry toluene (60 mL) in a 100 mL round-bottom flask, equipped with a stir bar, under inert Ar atmosphere. The solution was heated to 80 °C and stirred for 3 h. After cooling to room temperature, the mixture was passed through a short alumina column, and washed with CH_2Cl_2 and then with CH_2Cl_2/THF (5:1). The CH_2Cl_2/THF solvent was removed *in vacuo*. The solid was dissolved in hexanes, and silica gel column chromatography was used to isolate the product. Side products were eluted with hexanes/CH_2Cl_2 (3:1), and the dimer was eluted using pure CH_2Cl_2. The desired product dimer **3** was obtained as a black solid (30 mg, 60%). ^{1}H NMR ($CDCl_3$/1% d^5-pyridine, 200 MHz): δ 0.85 (t, 24 H, J = 6.7 Hz), 1.24 (m, 80 H), 1.72 (m, 16 H), 2.71 (t, 16 H, J = 7.2 Hz), 2.74 (s, 6 H), 7.02 (s, 4 H), 7.18 (s, 4 H), 7.34 (s, 8 H), 7.47 (d, 4 H, J = 4.5 Hz), 7.52 (d, 4 H, J = 4.5 Hz) 7.84 (d, 4 H, J = 8.1 Hz), 8.11 (d, 4 H, J = 8.1 Hz). ^{13}C NMR ($CDCl_3$/1% d^5-pyridine, 50 MHz): δ 14.05, 22.64, 29.33, 29.47, 29.69, 31.54, 31.89, 35.91, 117.87, 125.35, 126.88, 127.30, 129.88, 130.79, 132.91, 133.03, 136.01, 147.23, 152.03, 153.21, 153.53, 154.54, 197.96. IR (KBr, cm^{-1}): 2923 (s), 2852 (s), 1687 (m), 1599 (m), 1465 (m), 1264 (m), 1142 (m), 997 (w), 721 (w). UV−vis (THF, λ_{max}, nm): 422, 576. MALDI-TOF-MS m/z calcd for $C_{184}H_{254}N_8O_2Zn_2$ (M^+) 2735.8603; found, 2735.78.

AUTHOR INFORMATION

Corresponding Author

*Department of Chemistry, McMaster University, 1280 Main St., W. Hamilton, ON L8S 4M1. Tel: (905) 525-9140 x23514. Fax: (905) 521-2773. E-mail: adronov@mcmaster.ca.

ACKNOWLEDGMENT

Financial support for this work was provided by the Natural Science and Engineering Research Council (NSERC) of Canada, the Canada Foundation for Innovation (CFI), and the Ontario Innovation Trust (OIT). We also thank Professor Gianluigi Botton and the Canadian Centre for Electron Microscopy (CCEM) for assistance with TEM characterization of samples.

REFERENCES

(1) Kadish, K., Smith, K. M., Guilard, R., Eds. *The Porphyrin Handbook*; Academic Press: New York, 1999.
(2) Drain, C. M.; Varotto, A.; Radivojevic, I. *Chem. Rev.* **2009**, *109*, 1630–1658.
(3) Hasobe, T. *Phys. Chem. Chem. Phys.* **2010**, *12*, 44–57.
(4) Boyd, P. D. W.; Reed, C. A. *Acc. Chem. Res.* **2005**, *38*, 235–242.
(5) Guldi, D. M.; Rahman, G. M. A.; Zerbetto, F.; Prato, M. *Acc. Chem. Res.* **2005**, *38*, 871–878.
(6) Fukuzumi, S.; Kojima, T. *J. Mater. Chem.* **2008**, *18*, 1427–1439.
(7) Chitta, R.; D'Souza, F. *J. Mater. Chem.* **2008**, *18*, 1440–1471.
(8) Li, H. P.; Martin, R. B.; Harruff, B. A.; Carino, R. A.; Allard, L. F.; Sun, Y. P. *Adv. Mater.* **2004**, *16*, 896–900.
(9) Campidelli, S.; Sooambar, C.; Diz, E. L.; Ehli, C.; Guldi, D. M.; Prato, M. *J. Am. Chem. Soc.* **2006**, *128*, 12544–12552.
(10) Liu, Z. B.; Tian, J. G.; Guo, Z.; Ren, D. M.; Du, T.; Zheng, J. Y.; Chen, Y. S. *Adv. Mater.* **2008**, *20*, 511–515.
(11) Cheng, F. Y.; Adronov, A. *Chem. Mater.* **2006**, *18*, 5389–5391.
(12) Mickelson, E. T.; Huffman, C. B.; Rinzler, A. G.; Smalley, R. E.; Hauge, R. H.; Margrave, J. L. *Chem. Phys. Lett.* **1998**, *296*, 188–194.
(13) Sinnott, S. B. *J. Nanosci. Nanotechnol.* **2002**, *2*, 113–123.
(14) Britz, D.; Khlobystov, A. *Chem. Soc. Rev.* **2006**, *35*, 637–659.
(15) Murakami, H.; Nomura, T.; Nakashima, N. *Chem. Phys. Lett.* **2003**, *378*, 481–485.
(16) Li, H. P.; Zhou, B.; Lin, Y.; Gu, L. R.; Wang, W.; Fernando, K. A. S.; Kumar, S.; Allard, L. F.; Sun, Y. P. *J. Am. Chem. Soc.* **2004**, *126*, 1014–1015.
(17) Chen, J. Y.; Collier, C. P. *J. Phys. Chem. B* **2005**, *109*, 7605–7609.
(18) Hasobe, T.; Fukuzumi, S.; Kamat, P. V. *J. Am. Chem. Soc.* **2005**, *127*, 11884–11885.
(19) Guldi, D. M.; Taieb, H.; Rahman, G. M. A.; Tagmatarchis, N.; Prato, M. *Adv. Mater.* **2005**, *17*, 871–875.
(20) Saito, K.; Troiani, V.; Qiu, H. J.; Solladie, N.; Sakata, T.; Mori, H.; Ohama, M.; Fukuzumi, S. *J. Phys. Chem. C* **2007**, *111*, 1194–1199.
(21) Anderson, H. L.; Martin, S. J.; Bradley, D. D. C. *Angew. Chem., Int. Ed.* **1994**, *33*, 655–657.
(22) Screen, T. E. O.; Lawton, K. B.; Wilson, G. S.; Dolney, N.; Ispasoiu, R.; Goodson, T.; Martin, S. J.; Bradley, D. D. C.; Anderson, H. L. *J. Mater. Chem.* **2001**, *11*, 312–320.
(23) Screen, T. E. O.; Thorne, J. R. G.; Denning, R. G.; Bucknall, D. G.; Anderson, H. L. *J. Mater. Chem.* **2003**, *13*, 2796–2808.
(24) Cheng, F. Y.; Adronov, A. *Chem.—Eur. J.* **2006**, *12*, 5053–5059.
(25) Cheng, F. Y.; Adronov, A. *J. Porphyrins Phthalocyanines* **2007**, *11*, 198–204.
(26) Tsuda, A.; Furuta, H.; Osuka, A. *Angew. Chem., Int. Ed.* **2000**, *39*, 2549–2552.
(27) Tsuda, A.; Osuka, A. *Science* **2001**, *293*, 79–82.
(28) Tsuda, A.; Osuka, A. *Adv. Mater.* **2002**, *14*, 75–79.
(29) Cheng, F. Y.; Zhang, S.; Adronov, A.; Echegoyen, L.; Diederich, F. *Chem.—Eur. J.* **2006**, *12*, 6062–6070.
(30) Kamo, M.; Tsuda, A.; Nakamura, Y.; Aratani, N.; Furukawa, K.; Kato, T.; Osuka, A. *Org. Lett.* **2003**, *5*, 2079–2082.
(31) Holzinger, M.; Abraha, J.; Whelan, P.; Graupner, R.; Ley, L.; Hennrich, F.; Kappes, M.; Hirsch, A. *J. Am. Chem. Soc.* **2003**, *125*, 8566–8580.
(32) Wang, J. S.; Wai, C. M.; Shimizu, K.; Cheng, F.; Boeckl, J. J.; Maruyama, B.; Brown, G. *J. Phys. Chem. C* **2007**, *111*, 13007–13012.
(33) Chiang, I. W.; Brinson, B. E.; Huang, A. Y.; Willis, P. A.; Bronikowski, M. J.; Margrave, J. L.; Smalley, R. E.; Hauge, R. H. *J. Phys. Chem. B* **2001**, *105*, 8297–8301.
(34) Chiang, I. W.; Brinson, B. E.; Smalley, R. E.; Margrave, J. L.; Hauge, R. H. *J. Phys. Chem. B* **2001**, *105*, 1157–1161.